Paroxysmal Bundle Branch Block of Supraventricular Origin: A Possible Source of Misdiagnosis in Detecting Ventricular Tachycardia Using Time Domain Analyses of Intraventricular Electrograms

ROBERT D. THRONE, LORENZO A. DICARLO,* JANICE M. JENKINS, and STUART A. WINSTON*

From the Medical Computing Laboratory, Department of Electrical Engineering and Computer Science, University of Michigan, Ann Arbor, Michigan and *Cardiac Electrophysiology Laboratory, St. Joseph Mercy Hospital of the Catherine McAuley Health Center, Ann Arbor, Michigan

THRONE, R.D., ET AL.: Paroxysmal Bundle Branch Block of Supraventricular Origin: A Possible Source of Misdiagnosis in Detecting Ventricular Tachycardia Using Time Domain Analyses of Intraventricular Electrograms. *Current implantable antitachycardia devices use several methods for differentiating sinus rhythm (SR) from supraventricular tachycardia (SVT) or ventricular tachycardia (VT). These methods include sustained high rate, the rate of onset, changes in cycle length, and sudden onset. Additional methods for detecting VT include techniques based upon ventricular electrogram morphology. The morphological approach is based on the assumption that the direction of cardiac activation, as sensed by a bipolar electrode in the ventricle, is different when the patient is in SR as compared to VT. Whether paroxysmal bundle branch block of supraventricular origin (BBB) can be differentiated from VT has not been determined. In this study, we compared the morphology of the ventricular electrogram during sinus rhythm with a normal QRS (SR_{NlQRS}) or SVT with a normal QRS (SVT_{NlQRS}) with the morphologies of BBB and VT in 30 patients undergoing cardiac electrophysiology studies. Changes in ventricular electrogram morphology were determined using three previously proposed time domain methods for VT detection: Correlation Waveform Analysis (CWA), Area of Difference (AD), and Amplitude Distribution Analysis (ADA). CWA, AD, and ADA distinguished VT from SR_{NlQRS} or SVT_{NlQRS} in 16/17 (94%), 14/17 (82%), and 12/17 (71%) patients, and BBB from SR_{NlQRS} or SVT_{NlQRS} in 15/15 (100%), 13/15 (87%), and 6/15 (40%) patients, respectively. However, the ranges of values during BBB using these methods overlapped with ranges of values during VT in all cases for CWA, AD, and ADA. Hence, BBB may be a source of misdiagnosis in detecting VT when these time domain methods are used for ventricular electrogram analysis. (PACE, Vol. 13, April 1990)*

paroxysmal bundle branch block, correlation waveform analysis, area of difference, amplitude distribution analysis, tachycardia, ventricular tachycardia

Introduction

There are many proposed methods for the differentiation of sinus rhythm (SR) or supraventricular tachycardia (SVT) from ventricular tachycardia (VT) by antitachycardia devices. Most methods are based primarily on timing information, which has been implemented in the

This work was partially supported by NSF grant No. ECS-8351215 and a grant from Medtronic, Inc.

Address for reprints: Lorenzo A. DiCarlo, M.D., Reichert Health Building R-3003, Catherine McAuley Health Center, P.O. Box 994, Ann Arbor, MI 48106.

Received September 6, 1989; Revision December 7, 1989; Accepted January 3, 1990.

hardware available in such devices. The primary method for VT detection is based upon a sustained high rate of ventricular depolarizations. Other measurements derived from rate have also been studied for detecting VT including the difference between the rate changes during the onset of sinus tachycardia compared to those of VT[1] as well as changes in cycle length at the onset of VT[2] and rate stability during VT.[3] Among the methods most widely used for detection of VT in single chamber antitachycardia devices are combinations of rate, rate stability, and sudden onset.[4–10]

In addition to rate-related algorithms, methods of discriminating ventricular electrograms during SR from those during VT have been proposed for improving accuracy in VT detection. These include both time-domain and frequency-domain analyses. Frequency-domain analysis utilizes differences in frequency spectra between ventricular electrograms during SR and VT. Their use has had mixed results. Measurements of differences in the frequency with maximum power in the frequency domain, as well as the locations of the half-power (−3 dB) points in the frequency spectrum have not been uniformly successful.[11–13] After examining the amplitudes in frequency spectra at various power fall-off locations Pannizzo[13] proposed comparing amplitudes in frequency spectra of sinus rhythm and ventricular tachycardia depolarizations at the −12 dB point. However, these frequency domain methods have been applied only to a single ventricular depolarization from each class and the effect of variations over a number of ventricular depolarizations has not been examined.

Time-domain analyses utilize the information in the ventricular depolarizations directly, without any transformations to the frequency domain. The probability density function (PDF)[14,15] uses a measure of the amount of time a ventricular signal spends at baseline to discriminate SR or SVT from VT or ventricular fibrillation. The gradient pattern detection (GPD) algorithm[16] discriminates SR from VT based on the order in which the first derivative of the ventricular depolarization crosses predetermined thresholds. Use of differences in amplitude and slope (dV/dt) for discriminating SR from VT has not been successful.[17] Another method for detecting VT combines bandpass filtering, rectifying, amplitude scaling, and signal integration over a 5-second moving time window.[18] A feature extraction algorithm[19] utilizing the product of the peak amplitude difference (maximum–minimum) and duration (time between maximum and minimum) has been proposed but was tested on only four patients.

In this study, we examined three previously proposed time-domain methods for distinguishing VT from SR based on ventricular electrogram morphology: Correlation Waveform Analysis (CWA),[12,20] Area of Difference (AD),[11,17,21] and Amplitude Distribution Analysis (ADA).[10,12,22]

CWA distinguishes SR from VT by comparing a template created from normal ventricular depolarizations during SR with subsequent ventricular depolarizations using the correlation coefficient. CWA is independent of amplitude variations and baseline changes and depends primarily on the relative shape differences between the template and the waveform under analysis.

AD distinguishes SR from VT by comparing a template of normal ventricular depolarizations created during SR with subsequent ventricular depolarizations using the sum of the absolute difference between each sample point in the template and each point in the waveform under analysis. This method depends on amplitude differences between the template and waveform under analysis. Like CWA, the AD template matching method utilizes a binary decision which assumes that a close match between the derived template and subsequent depolarizations represents sinus rhythm.

ADA, a digital variant of the PDF method, does not utilize a template. Rather it measures the percentage of time a waveform spends near baseline and is based on the assumption that the amount of time spent at baseline in each cardiac cycle is significantly longer during sinus rhythm or supraventricular tachycardia than during VT. Lin et al.[12] found limited value in this method for discriminating VT from sinus rhythm with or without chronic bundle branch block using 5-point bins and dividing the peak-to-peak range of the signal into 30 intervals. Ripley et al.[10] found better separation between SR and VT using 5- and 7-point bins and dividing the peak-to-peak range into 32 intervals.

While all three of these time-domain methods have been successful in discriminating VT from SR in humans, the impact of paroxysmal bundle branch block of supraventricular origin has not been examined. The purpose of this study, therefore, was to determine whether BBB can be distinguished from sinus rhythm with a normal QRS (SR_{NlQRS}), supraventricular tachycardia with a normal QRS (SVT_{NlQRS}), and VT using these time-domain analyses.

Methods and Materials

Electrophysiology Study

Bipolar ventricular endocardial electrograms were recorded during elective clinical cardiac electrophysiology studies of 19 men and 11 women (age 14 to 84 years) with a normal QRS (<120 msec) during SR or SVT. Bundle branch block of supraventricular origin was induced in 15 of the patients (11 RBBB, 4 LBBB), and monomorphic VT was induced in 17 of the patients. Two patients were common to both groups. Patient information and results are given in Tables I and II.

Patients were studied in a fasting postabsorptive state after sedation with 1–3 mg of intravenous medazolam. After administering 1% lidocaine for local anesthesia, three 7 French sidearm sheaths (Cordis Corp., Miami, FL, USA) were positioned in the right femoral vein using the Seldinger technique. Three 6 French quadrapolar electrode catheters with an interelectrode distance of 1 cm (USCI division, C.R. Bard Inc., Billerica, MA, USA) were introduced and advanced under fluoroscopic guidance to the high right atrium, tricuspid valve for His-bundle recording, and right ventricular apex. All recordings were made with the patients lying supine. Immediately before programmed stimulation a 12-lead electrocardiogram was recorded during SR. Ventricular electrograms were recorded on FM tape (Hewlett Packard 3968 and 3964A, Hewlett Packard, San Diego, CA, USA) with filter settings of 0.5 to 500

Table I.

Patient Data for SR vs. VT

Patient	Heart Disease	Drugs	VT Morphology	CWA	AD	ADA 5 pt bin	ADA 7 pt bin
1	CAD	Proc	RBB-S	+	+	–	–
2	CAD	Proc	RBB-I	+	+	–	+
3	CAD	Proc	RBB-I	+	+	+	+
4	CAD	Proc	RBB-S	+	+	+	+
5	CAD	Proc	RBB-S	+	+	+	+
6	CAD	Qu Me	LBB-S	+	–	+	+
7	CAD	Am	RBB-S	–	–	+	+
8	CAD	None	LBB-S	+	+	+	+
9	CAD	None	RBB-S	+	+	+	+
10	CAD	None	RBB-S	+	+	–	–
11	CAD	None	RBB-I	+	–	–	–
12	CAD	None	RBB-I	+	+	+	+
13	CAD	None	IND-S	+	+	+	+
14	CAD	None	RBB-S	+	+	+	+
15	None	None	LBB-S	+	+	+	+
16	None	None	RBB-S	+	+	–	–
17	None	Iso	LBB-I	+	+	–	–

'+' = no overlap in the ranges for the two rhythms, '–' = some overlap in the ranges for the two rhythms; CWA = Correlation Waveform Analysis, AD = Area of Difference, ADA = Amplitude Distribution Analysis; CAD = Coronary Artery Disease; Am = Amiodarone, Iso = Isopril, Me = Mexilitine, Qu = Quinidine, Proc = Procainamide; IND = indeterminant, LBB = left bundle branch, RBB = right bundle branch; S = Superior, I = Inferior.

Table II.

Patient Data for SR vs. BBB

Patient	Heart Disease	Drugs	Method of BBB Induction	Aberration Morphology	CWA	AD	ADA 5 pt bin	ADA 7 pt bin
18	None	None	Spontaneous	RBBB	+	+	+	+
19	None	None	AOP	RBBB	+	–	–	–
20	None	None	AOP	RBBB	+	+	+	+
16	None	None	Spontaneous	RBBB	+	+	–	–
21	None	Iso	AOP	RBBB	+	+	–	–
22	None	Iso	Atrial Fibrillation	RBBB	+	+	–	+
23	None	Iso	Spontaneous	RBBB	+	+	+	+
24	COPD	None	AOP	RBBB	+	–	–	–
25	CAD	None	Spontaneous	RBBB	+	+	–	–
26	CAD	None	AOP	RBBB	+	+	+	+
1	CAD	Proc	AOP	RBBB	+	+	–	+
27	None	None	ORT	LBBB	+	+	–	–
28	None	Iso	AOP	LBBB	+	+	–	–
29	None	Proc	ORT	LBBB	+	+	–	–
30	CAD	None	AOP	LBBB	+	+	–	–

'+' = no overlap in the ranges for the two rhythms, '–' = some overlap in the ranges for the two rhythms; CWA = Correlation Waveform Analysis, AD = Area of Difference, ADA = Amplitude Distribution Analysis; CAD = Coronary Artery Disease, COPD = Chronic Obstructive Pulmonary Disease; Iso = Isopril, Proc = Procainamide; LBBB = left bundle branch block, RBBB = right bundle branch block; AOP = atrial overdrive pacing, ORT = orthodromic reciprocating tachycardia.

Hz (Siemens Mingograf-7, Siemens, Solna, Sweden) and 1 to 500 Hz (Honeywell, Electronics for Medicine, Pleasantville, NY, USA). Tape speed was $3\frac{3}{4}$ inches per second with a bandwidth of 0–1,250 Hz. The recorded ventricular electrograms were subsequently digitized on an IBM PC/AT with a Tecmar Lab Master (Scientific Solutions, Inc.,) analog-to-digital system at a sampling rate of 1,000 Hz. The programs for digitization and subsequent waveform analysis were written in C programming language and assembly language.

Methods of Analysis

Data sets consisted of three 15 second passages from each patient. Two separate passages were digitized from recordings made during sinus rhythm with a normal QRS in 28 patients, and during SVT with a normal QRS in two patients (patients 21 and 29). The two patients with a normal QRS during SVT (SVT_{NIQRS}) had an orthodromic reciprocating tachycardia. BBB occurred when the cycle length of the SVT decreased by 60 and 80 msec, respectively. The heart rate recorded during the first two passages was similar for each patient. A third passage was digitized from a segment recorded during induced monomorphic VT or during BBB.

The first passage of SR_{NIQRS} or SVT_{NIQRS} was used to construct a template for subsequent comparison with the second passage of SR_{NIQRS} or SVT_{NIQRS} and a passage of VT or BBB. The template was constructed by signal averaging depolarizations and was chosen to include only depolarization as described previously.[23] This template was then used for the correlation waveform analysis and the area of difference methods. A software trigger was used for detection of waveforms. For both CWA and AD methods, a best fit algorithm[23] was used to align the templates with the waveforms under analysis in the following manner. Templates were initially aligned with the depolarization under analysis using the maximum departure from baseline and both the correlation coefficient and the area of difference were computed. The waveform under analysis was then shifted in a stepwise fashion to the left, recalculating the correlation coefficient and the area of difference at each sample point within a

5-msec window, and similarly to the right for each sample point within a 5-msec window. The maximum correlation within the sliding window was the indicator of best alignment and was taken to be the correlation coefficient for that depolarization. Similarly, the minimum value of the area of difference was taken to be the area of difference for that depolarization.

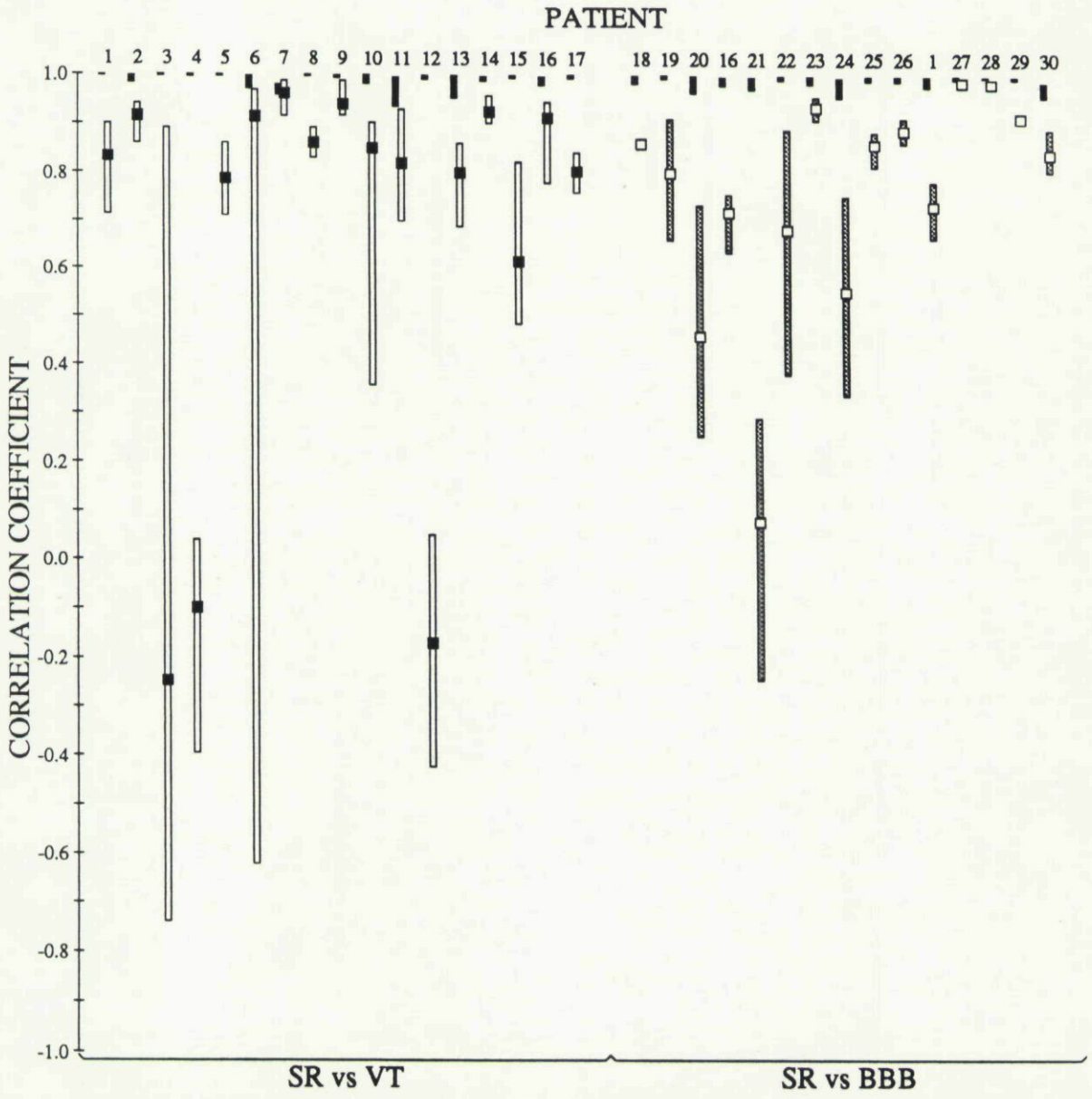

Figure 1. *Derived ranges of correlation coefficient during sinus rhythm with a normal QRS (SR_{NlQRS}) or supraventricular tachycardia with a normal QRS (SVT_{NlQRS}) compared to ventricular tachycardia (VT) and bundle branch block of supraventricular origin (BBB). The ranges of correlation coefficient during VT overlap with the ranges for BBB. SR_{NlQRS} or SVT_{NlQRS} is black, VT is white, BBB is shaded. Mean values for VT are black squares, while the mean values for BBB are white squares. Mean values for SR_{NlQRS} or SVT_{NlQRS} are not displayed due to the small variation.*

Correlation Waveform Analysis (CWA)

Correlation waveform analysis[12,20] computes the correlation coefficient (ρ) between a template and the waveform under analysis. The value of the correlation coefficient falls between ±1 such that identical signals have a value of +1, signals which are inverses of one another have a value of −1, and dissimilar signals fall within that range. Mathematically, the correlation coefficient is defined as

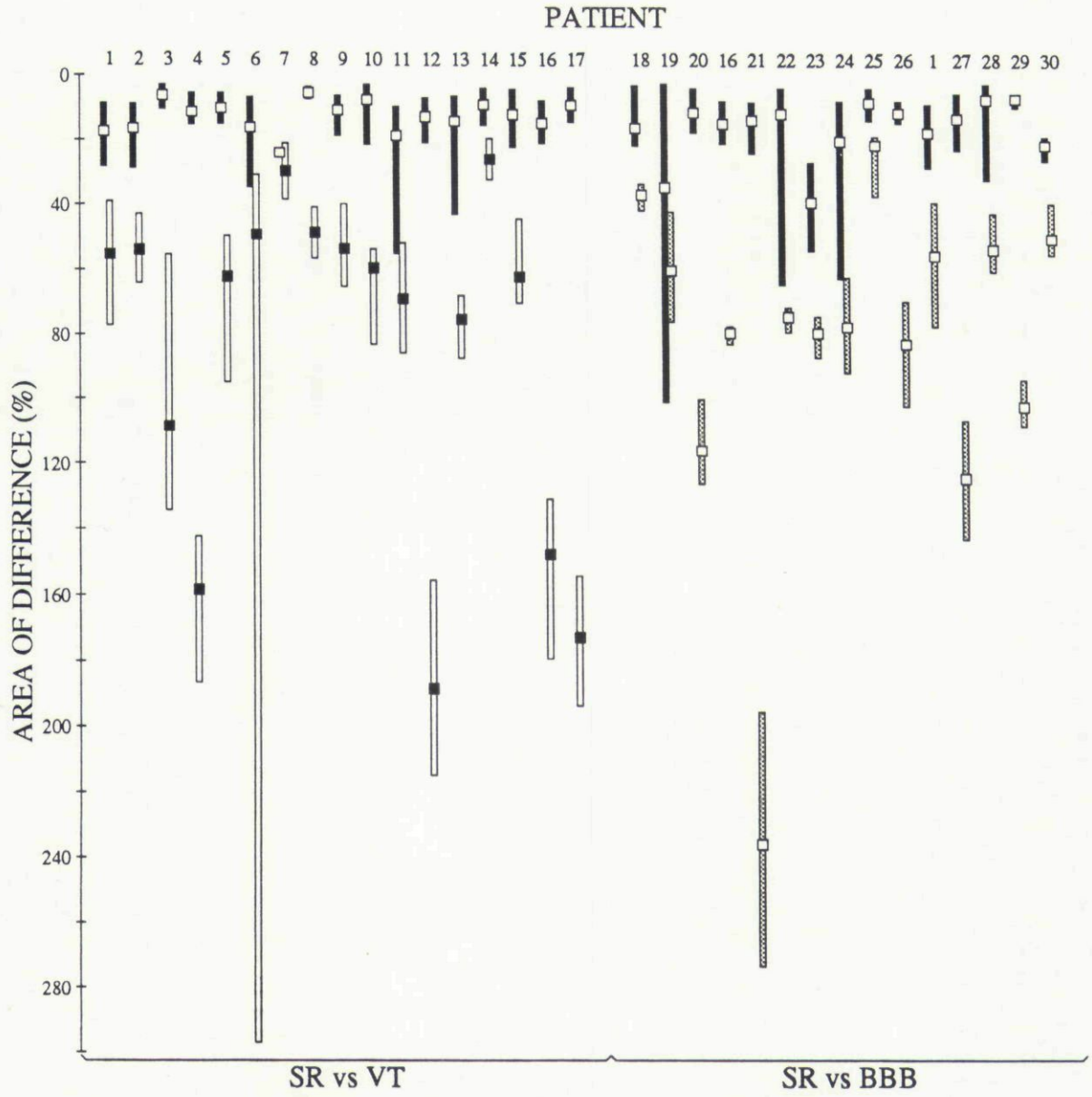

Figure 2. *Derived ranges of area of difference during sinus rhythm with a normal QRS (SR_{NlQRS}) or supraventricular tachycardia with a normal QRS (SVT_{NlQRS}) compared to ventricular tachycardia (VT) and bundle branch block of supraventricular origin (BBB). Area of difference values are expressed as a percentage of the total area between the SR_{NlQRS} or SVT_{NlQRS} template and the isoelectric line. The ranges of the area of difference during VT overlap with the ranges for BBB. SR_{NlQRS} or SVT_{NlQRS} is black, VT is white, BBB is shaded. Mean values for VT are black squares, while the mean values for BBB and SR_{NlQRS} or SVT_{NlQRS} are white squares.*

$$\rho = \frac{\sum_{i=1}^{i=N} (T_i - \bar{T})(S_i - \bar{S})}{\sqrt{\sum_{i=1}^{i=N} (T_i - \bar{T})^2} \sqrt{\sum_{i=1}^{i=N} (S_i - \bar{S})^2}}$$

where ρ = the correlation coefficient; N = the number of template points; T_i = the template points; S_i = the signal points under analysis; $\bar{T}$ = the average of the template points; $\bar{S}$ = the average of the signal points.

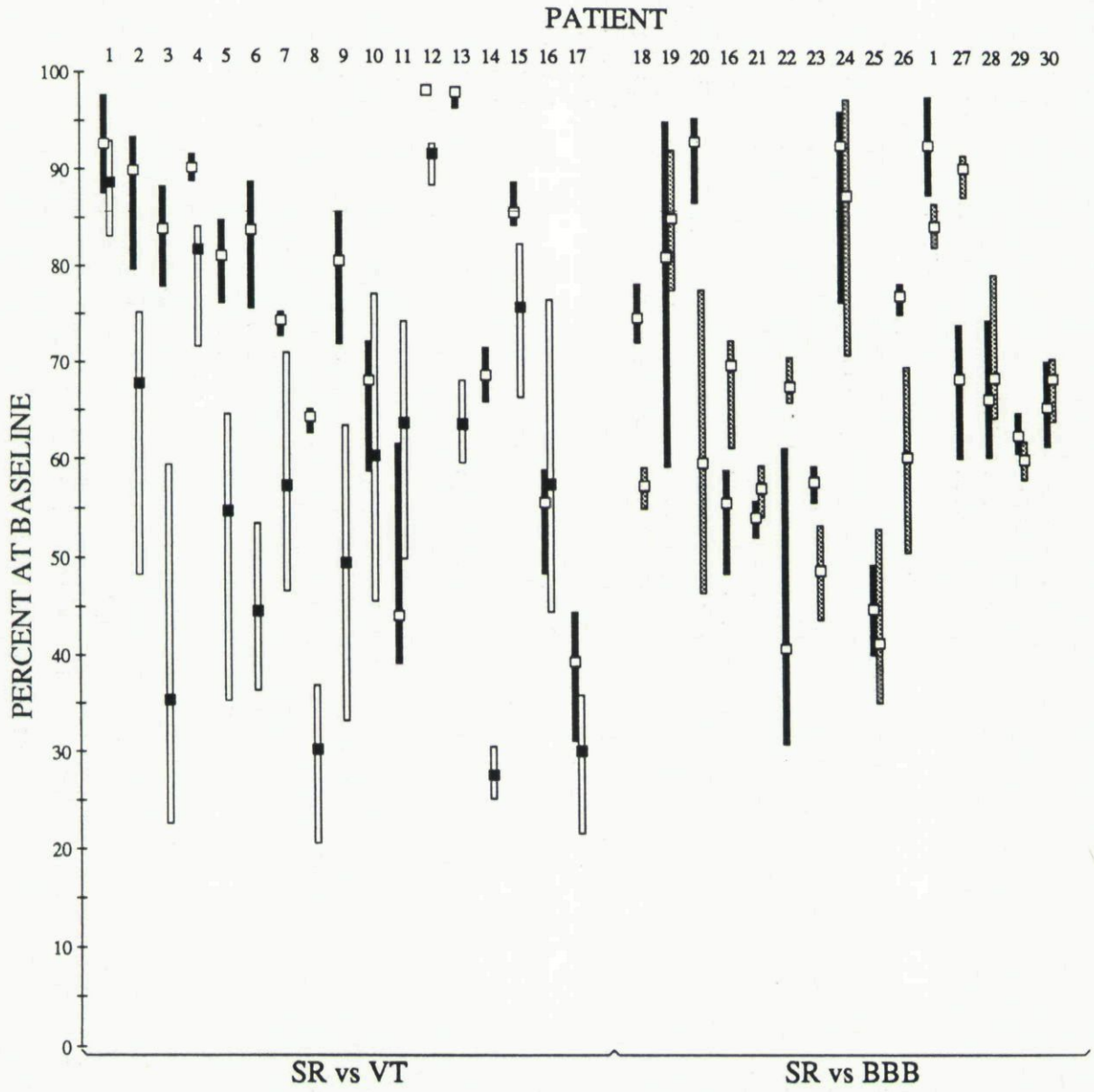

Figure 3. *Derived ranges of amplitude distribution analysis during sinus rhythm with a normal QRS (SR_{NlQRS}) or supraventricular tachycardia with a normal QRS (SVT_{NlQRS}) compared to ventricular tachycardia (VT) and bundle branch block of supraventricular origin (BBB). The ranges of the amplitude distribution during VT overlap with the ranges for BBB, is black, VT is white, BBB is shaded. Mean values for VT are black squares, while the mean values for BBB and SR_{NlQRS} or SVT_{NlQRS} are white squares.*

The correlation coefficient is independent of amplitude fluctuations and measures only relative shape differences between the template and the waveform being examined.[24]

Area of Difference (AD)

The area of difference,[11,17,21] directly measures the absolute difference in amplitude of sample points of the template and the waveform under analysis and normalizes the result by the value of the template. Mathematically,

$$AD = \sum_{i=1}^{i=N} |T_i - S_i|$$

N = the number of template points; T_i = the template points; S_i = the signal points under analysis. The area of difference is usually reported as a percentage change of the absolute deviation of the template points from the baseline, i.e.,

$$AD(\%) = \frac{\sum_{i=1}^{i=N} |T_i - S_i|}{\sum_{i=1}^{i=N} |T_i|} \times 100\%$$

This method uses information contained in differences in amplitude between ventricular electrograms during sinus rhythm and VT.

Amplitude Distribution Analysis (ADA)

Amplitude distribution analysis[10,12,22] computes the total amount of time spent at baseline. In this method the peak-to-peak amplitude of the signal is divided into 32 equally sized ranges (bins), and the number of sample points of an entire cardiac cycle falling within each range is computed. Thus a histogram is created that reflects the distribution of amplitude of each of the

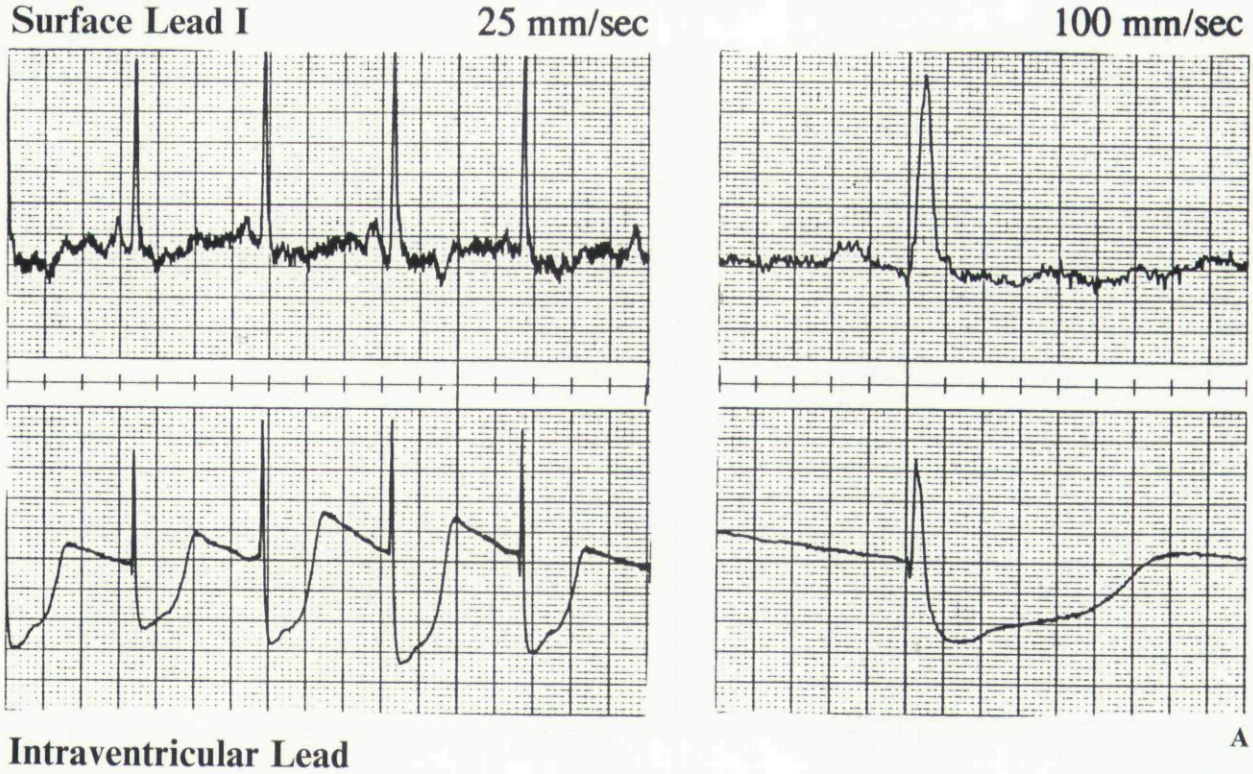

Figure 4. *Typical depolarizations (surface lead I and the intraventricular lead) for patient 16 at paper speeds of 25 mm/sec and 100 mm/sec. The passages were recorded and displayed at identical gain settings. (A) Normal sinus rhythm. (B) Right bundle branch aberration. (C) Ventricular tachycardia with a right bundle branch superior axis morphology. The intraventricular electrogram during both the right bundle branch aberration and the ventricular tachycardia were essentially of opposite polarity than the ventricular electrogram during normal sinus rhythm.*

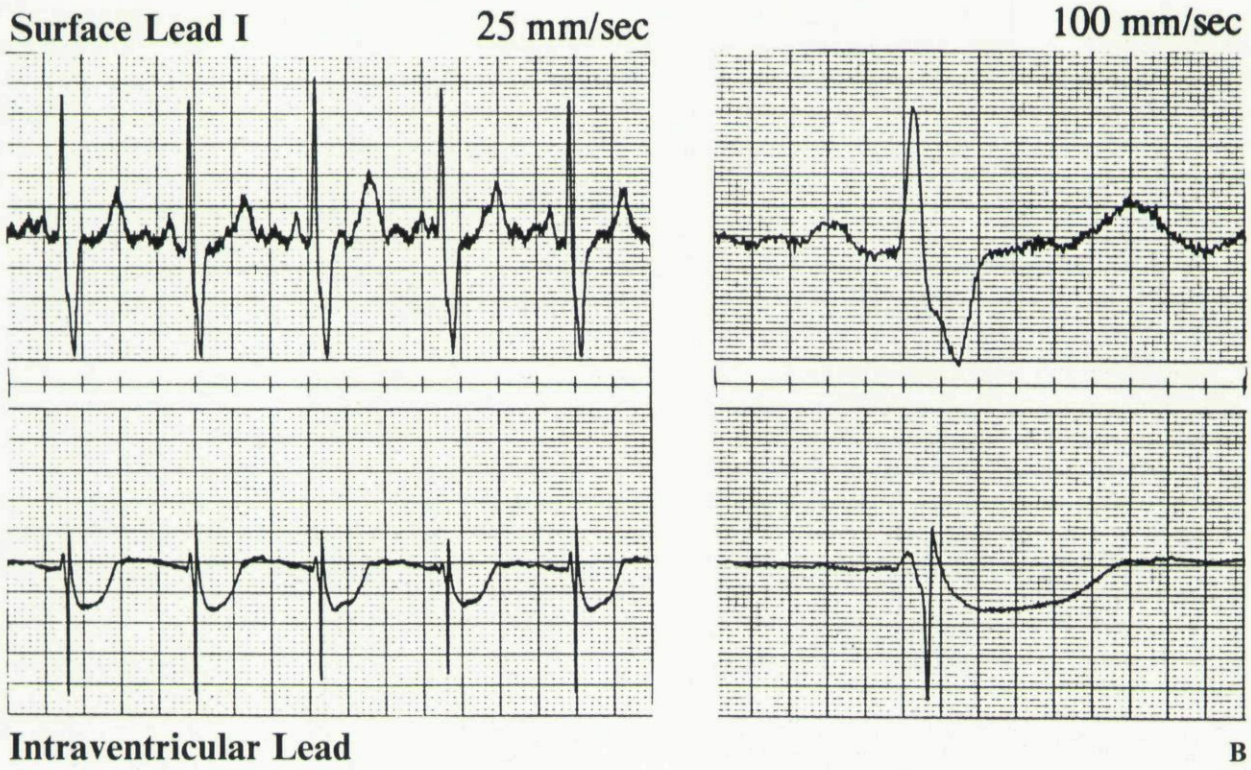

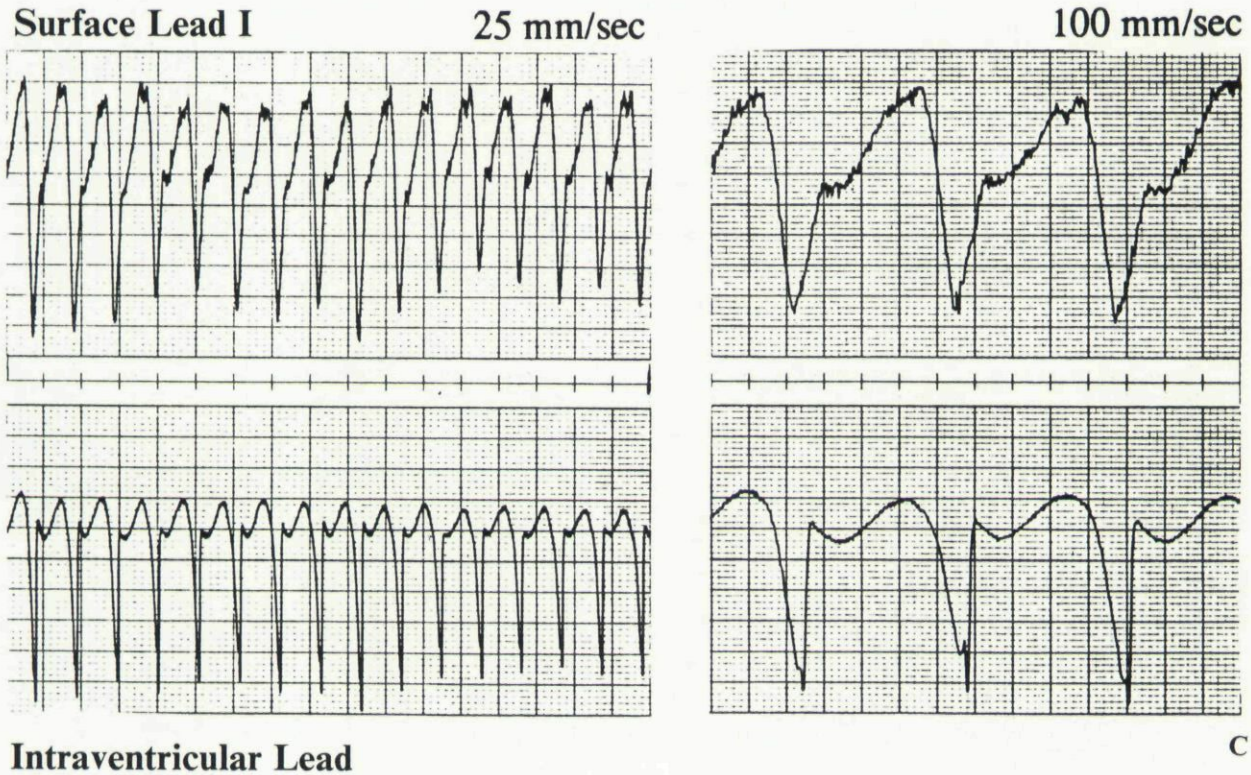

Figure 4. *Continued*

digitized sample points. The percentage of time at baseline for each cardiac cycle is estimated by the number of points that fall within the bin with the majority of points and the two adjacent bins on either side (making a 5-point bin) or three adjacent bins on either side (making a 7-point bin).

Results

Qualitative results of using CWA, AD, and ADA for the 30 patients are given in Tables I and II. Table I lists the patient, heart disease, drugs during the study, and the morphology of the VT. A '+' indicates that the ranges of values during SR_{NlQRS} or SVT_{NlQRS} could be distinguished from the ranges of values during VT, while a '−' indicates some overlap in the ranges. Table II lists the patient, existing heart disease, drugs present during the study, the circumstances under which BBB occurred, and the morphology of the aberration (LBBB or RBBB). A '+' indicates that the range of values during SR_{NlQRS} or SVT_{NlQRS} could be distinguished from the range of values during BBB, while a '−' indicates some overlap in the ranges. In the majority of instances the range of values determined for SR, VT, and BBB was generally symmetric about the mean. Skewing of the range was occasionally affected by fusion depolarizations.

Correlation Waveform Analysis

Figure 1 displays the quantitative results using correlation waveform analysis. Results for each patient are displayed in a column located on

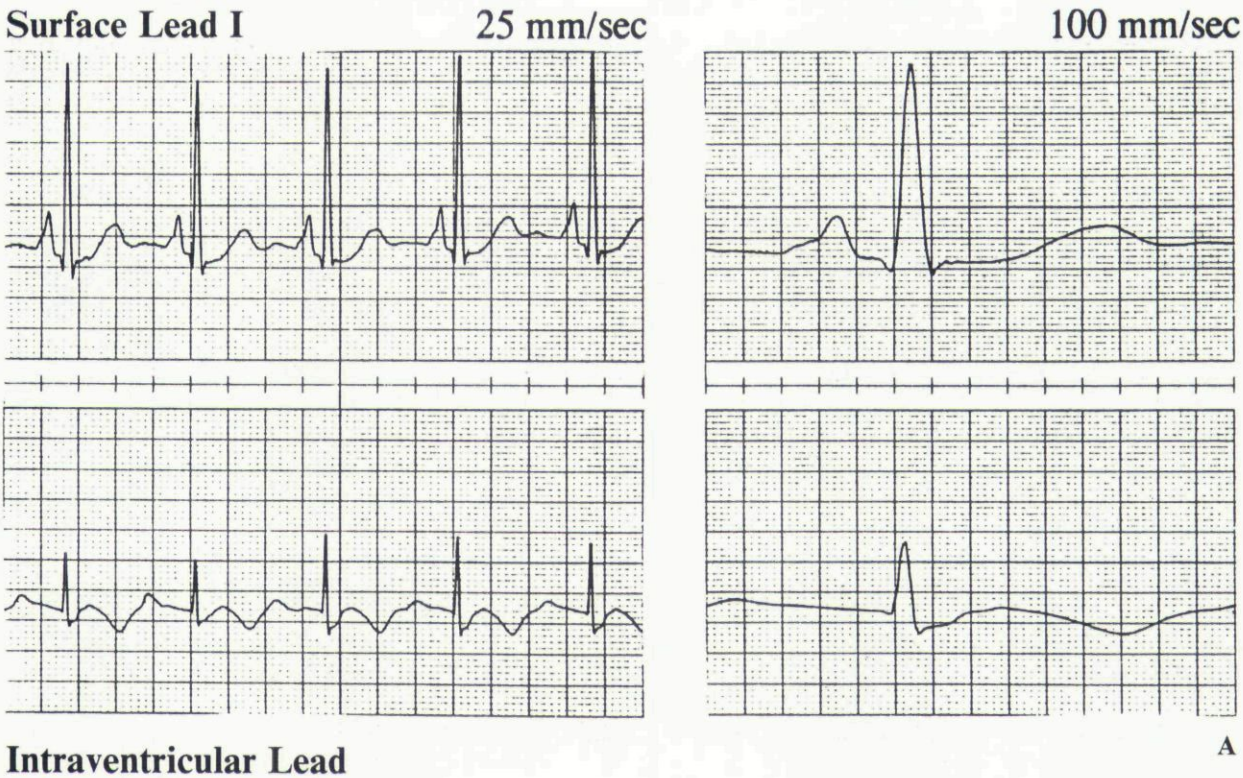

Figure 5. *Typical depolarizations (surface lead I and the intraventricular lead) for patient 27 at paper speeds of 25 mm/sec and 100 mm/sec. The passages were recorded and displayed at identical gain settings. (A) Supraventricular tachycardia with a normal QRS. (B) Left bundle branch aberration. This patient had a concealed accessory atrioventricular pathway. The patient had a normal QRS during orthodromic reciprocating tachycardia and subsequently developed left bundle branch block.*

the horizontal axis. Below each patient identifier, the range of values of the correlation coefficients (ρ) and the mean value for each passage (the ranges of correlation coefficients for SR are generally so small the mean is not plotted) are displayed along the vertical axis for SR_{NlQRS} or SVT_{NlQRS}, VT, and BBB. CWA distinguished VT from SR_{NlQRS} or SVT_{NlQRS} in 16/17 (94%) patients with complete separation, and BBB from SR_{NlQRS} or SVT_{NlQRS} in 15/15 (100%) patients. However, ranges of values computed in BBB considerably overlapped with the ranges of those in VT.

Area of Difference

Figure 2 displays the quantitative results using the area of difference method. Results for each patient are displayed in a column located on the horizontal axis. Below each patient identifier, the range of values of the area of difference and the mean value for each passage are displayed along the vertical axis for VT and BBB. AD distinguished VT from SR_{NlQRS} or SVT_{NlQRS} in 14/17 (82%) patients, and BBB from SR_{NlQRS} or SVT_{NlQRS} in 13/15 (87%) patients, but in this method as well the ranges of BBB and VT overlapped.

Amplitude Distribution Analysis

Figure 3 displays the quantitative results using amplitude distribution analysis using the 7-point bins, which performed better than the 5-point bins. The underlying assumption of ADA is that ventricular depolarization during SR_{NlQRS} or SVT_{NlQRS} will spend more time at 'baseline' than during VT or BBB. Hence if the ranges of amplitude distribution during BBB or VT did not overlap with the ranges during SR_{NlQRS} or SVT_{NlQRS}, but the ranges during SR_{NlQRS} or SVT_{NlQRS} were lower than for VT or BBB (i.e., the waveform was spending more time at baseline during BBB or VT than during SR_{NlQRS} or SVT_{NlQRS}), then ADA was declared to have failed. Results for each patient are displayed in a column located on the horizon-

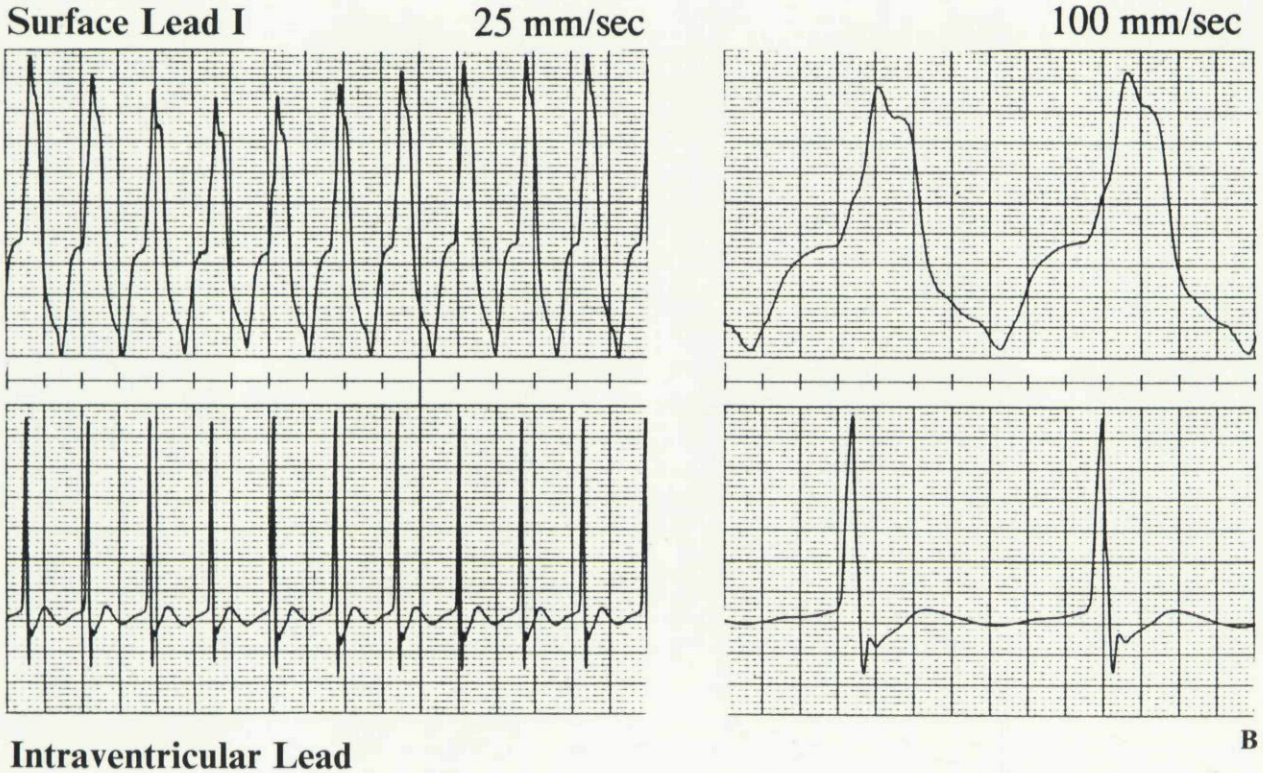

Figure 5. *Continued*

tal axis. Below each patient identifier, the ranges of the values of the amplitude distribution and the mean value for each passage of SR_{NIQRS} or SVT_{NIQRS}, VT, and BBB are displayed. ADA could distinguish VT from SR_{NIQRS} or SVT_{NIQRS} in 12/17 (71%) patients, and BBB from SR_{NIQRS} or SVT_{NIQRS} in 6/15 (40%) patients. Again the ranges of BBB and VT overlap.

Typical passages during sinus rhythm, ventricular tachycardia, and right and left bundle branch block aberration are shown in Figures 4–7. The passages are displayed at both 25 mm/sec and 100 mm/sec. All intraventricular electrograms for a single patient were recorded and displayed with identical gain settings. Similarly, all surface leads were recorded and displayed with identical gain settings for a single patient. Figure 4 contains passages from patient 16, who developed right bundle branch aberration and also had monomorphic VT induced. The polarity of the ventricular electrogram during both VT and BBB was essentially of opposite polarity to the ventricular electrogram during normal sinus rhythm. Figure 5 contains passages from patient 27, who developed left bundle branch block during a supraventricular tachycardia. Figure 6 contains passages from patient 18, who developed right bundle branch aberration. The change in the ventricular electrogram between sinus rhythm and the right bundle branch aberration was not as pronounced as for patient 16 (Fig. 4). Finally, Figure 7 contains passages from patient 3, who had monomorphic ventricular tachycardia induced. The ventricular electrograms during VT were of opposite polarity to those during sinus rhythm.

Discussion

In this study, we compared the morphology of the ventricular electrograms during SR_{NIQRS} or

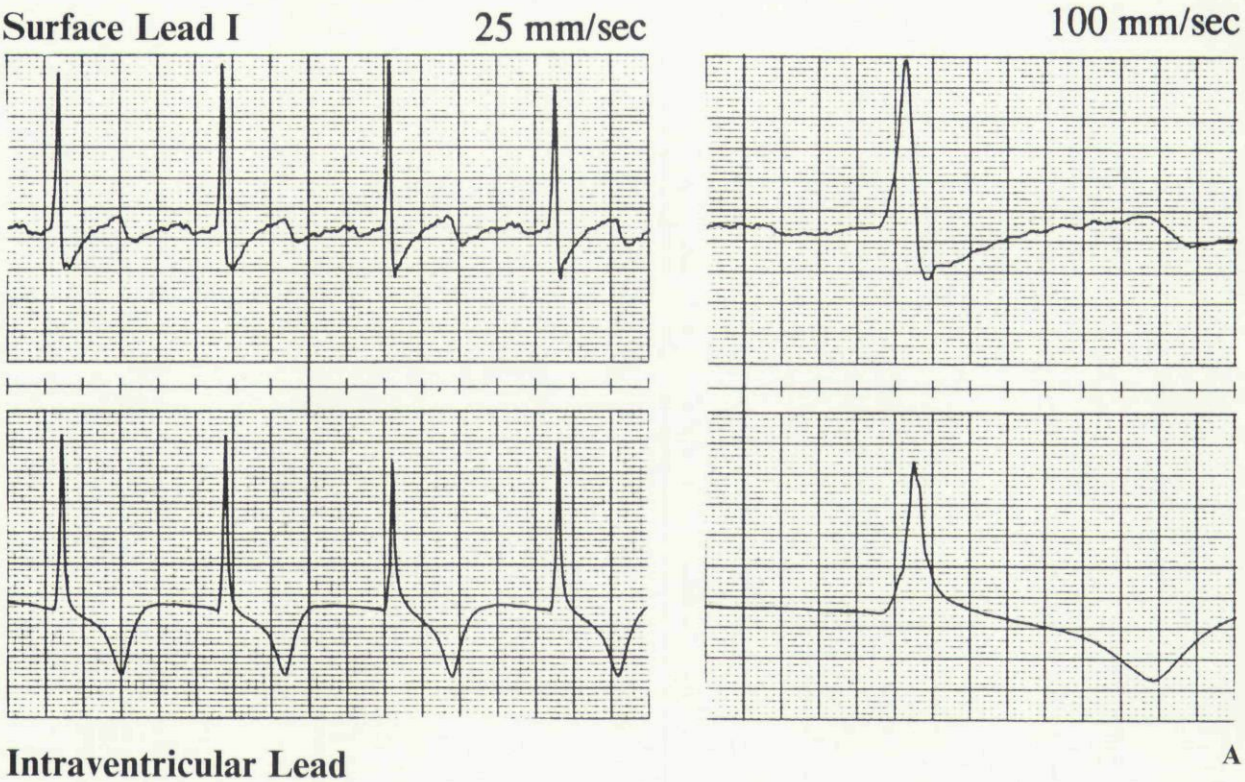

Figure 6. *Typical depolarizations (surface lead I and the intraventricular lead) for patient 18 at paper speeds of 25 mm/sec and 100 mm/sec. The passages were recorded and displayed at identical gain settings. (A) Normal sinus rhythm. (B) Right bundle branch aberration. The intraventricular electrograms during both the right bundle branch block aberration and normal sinus rhythm were of the same polarity.*

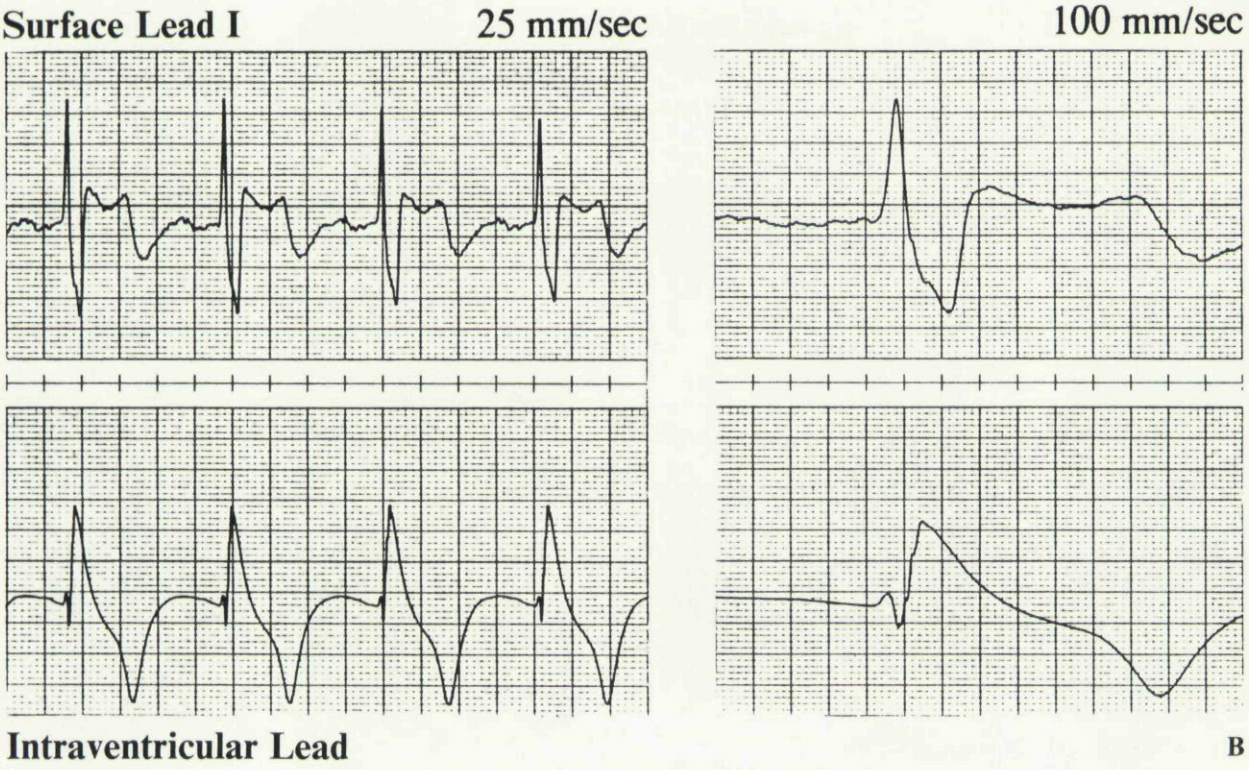

Figure 6. *Continued*

SVT_{NIQRS} with the morphologies of BBB and VT using three previously proposed time-domain methods for discriminating sinus rhythm from VT: correlation waveform analysis, area of difference, and amplitude distribution analysis. CWA, AD, and ADA using 7-point bins distinguished VT from SR_{NIQRS} or SVT_{NIQRS} in 16/17 (94%), 14/17 (82%), and 12/17 (71%) patients, respectively. CWA, AD, and ADA using 7-point bins distinguished BBB from SR_{NIQRS} or SVT_{NIQRS} in 15/15 (100%), 13/15 (87%), and 6/15 (40%) patients, respectively.

In the two patients with both VT and BBB induced, VT could be distinguished from BBB and SR_{NIQRS} using both CWA and AD in one patient (patient 16), but not in the other (patient 1). For patient 16 (Fig. 4), SR_{NIQRS} and subsequently induced BBB and VT could be distinguished from each other using both CWA and AD. Using CWA, the ranges for VT and SR_{NIQRS} were closer than those for BBB versus SR_{NIQRS}, while with AD the ranges for BBB were closer to SR_{NIQRS}.

There was no single, derived value from correlation waveform analysis, area of difference, or amplitude distribution analysis which could differentiate all passages of VT from all passages of supraventricular BBB in our patient population. In some cases, ventricular electrograms during induced bundle branch block may display many of the characteristics of ventricular electrograms during VT, including changes in polarity (Fig. 4). This suggests that supraventricular tachycardia with aberrant conduction could confound these detection algorithms and potentially be misdiagnosed as VT.

There have been few attempts to differentiate the ventricular electrograms of VT from those of BBB reported in the literature. The use of CWA for differentiating ventricular electrograms during ventricular tachycardia from the ventricular electrograms of sinus rhythm with either a normal QRS or chronic bundle branch block in humans has previously been reported.[12] The effects of the presence of paroxysmal bundle branch block on detection methods based on ventricular morphology has previously been exam-

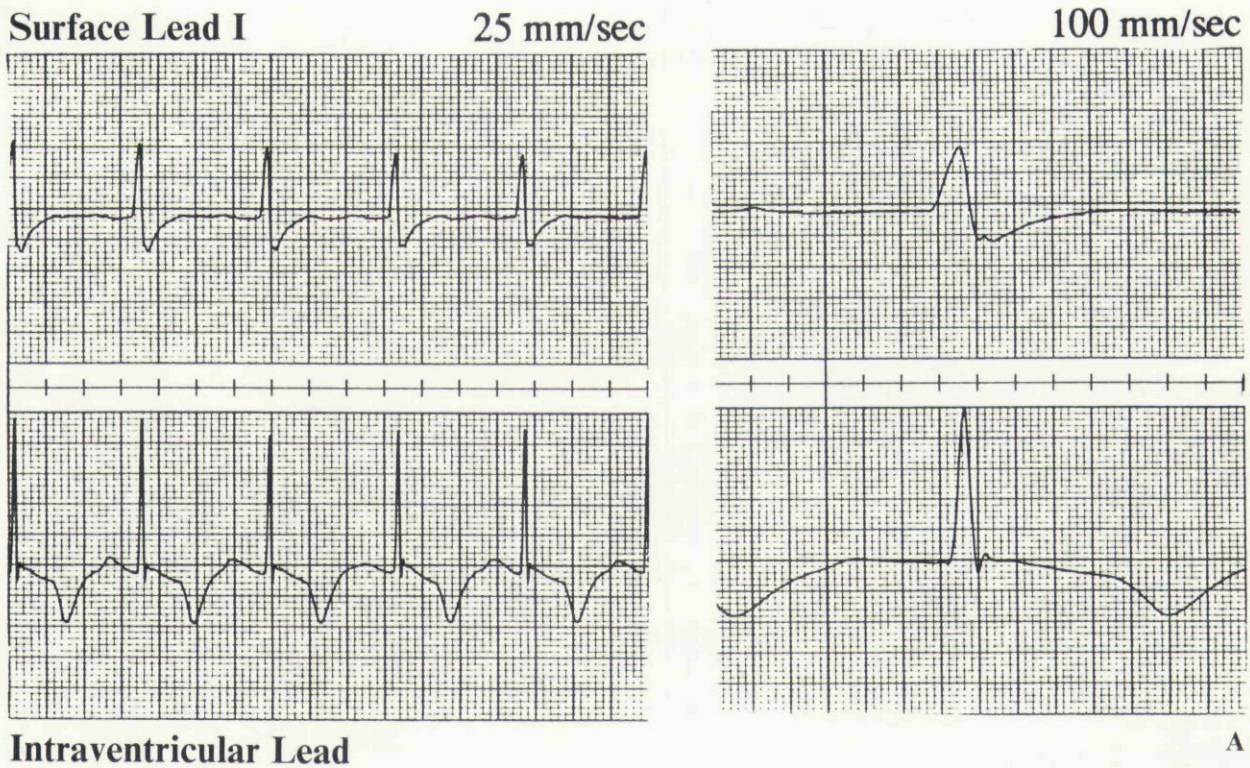

Figure 7. *Typical depolarizations (surface lead I and the intraventricular lead) for patient 3 at paper speeds of 25 mm/sec and 100 mm/sec. The passages were recorded and displayed at identical gain settings. (A) Normal sinus rhythm. (B) Ventricular tachycardia with a right bundle branch inferior axis morphology. The intraventricular electrograms during the ventricular tachycardia and normal sinus rhythm were of opposite polarity.*

ined only in canine hearts.[21] The potential use of templates made from induced, paroxysmal BBB has previously been suggested as a means to improve reliable detection of VT.[17] This method might be feasible if bundle branch aberration could reliably be induced during the electrophysiology study or during implantation of an antitachycardia device. However, this may not be possible. Paroxysmal bundle branch block could also potentially develop late after implantation due to changes in structural heart disease or in antiarrhythmic drug therapy.

The potential number of patients upon whom the findings of the present study might have an impact is difficult to determine. Based upon a retrospective review of 136 consecutive patients with inducible, sustained, monomorphic ventricular tachycardia during electrophysiological testing, paroxysmal bundle branch block of supraventricular origin has also been induced or observed in 5.3%.[25] However, this observed incidence of paroxysmal bundle branch block during electrophysiological testing may be an underestimate of its actual incidence when spontaneous changes in heart rate, autonomic tone, and/or myocardial oxygenation occur outside of the electrophysiology laboratory.

The present study was done using leads positioned acutely during electrophysiology studies. Template size was constrained by the need to exclude injury current typically present when using such leads. It is possible that a wider template size, which incorporates ventricular depolarization as well as repolarization, could be employed for chronic leads and might result in improved discrimination of BBB from VT. The results of amplitude distribution analysis may have been related to the acute injury current caused by our

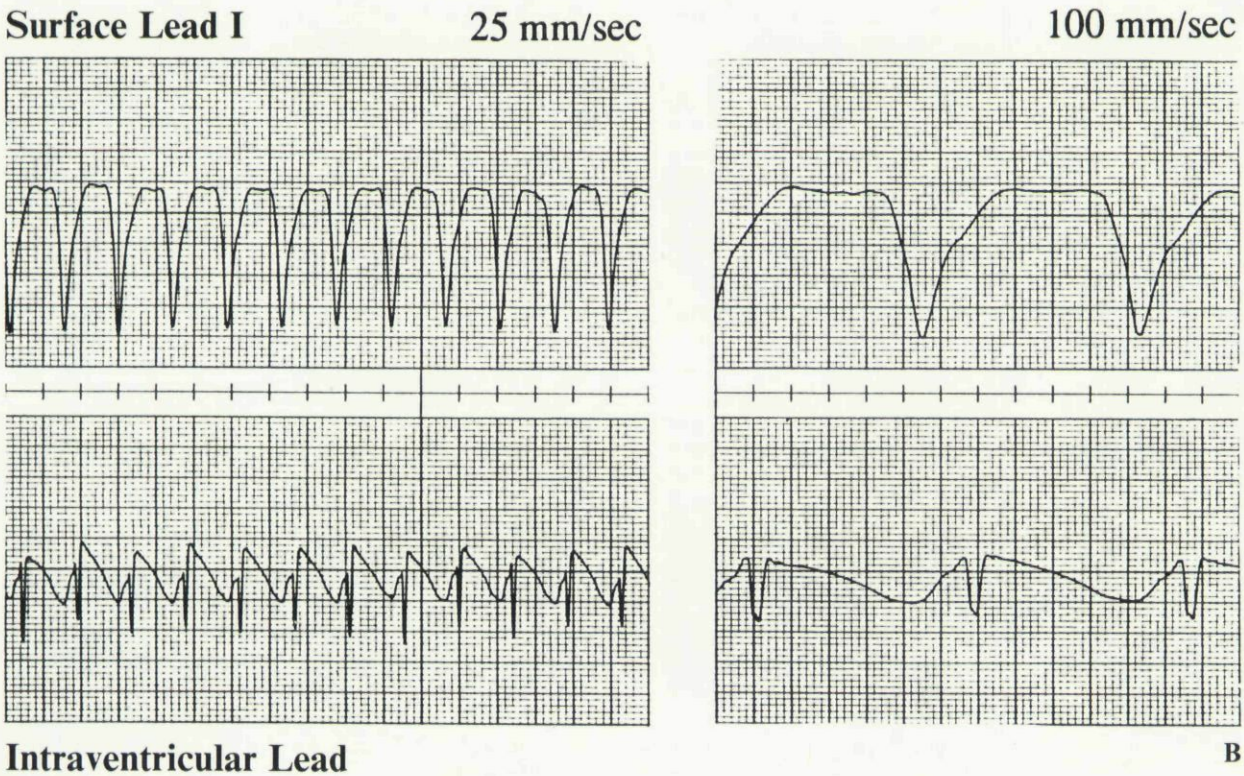

Figure 7. *Continued*

temporary leads that would be expected to subside once permanent leads are used.

Conclusion

In this study, we compared the morphology of the ventricular electrograms during SR_{NlQRS} or SVT_{NlQRS} with the morphologies of BBB and VT using three time-domain methods proposed for detecting VT: correlation waveform analysis, area of difference, and amplitude distribution analysis. CWA and AD appear to be reliable for distinguishing SR_{NlQRS} or SVT_{NlQRS} from either monomorphic VT or BBB. ADA was not quite as effective in distinguishing SR_{NlQRS} or SVT_{NlQRS} from VT, but appeared less likely to misdiagnose BBB as VT. However, for all three algorithms, reliable separation of BBB from VT could not be demonstrated. Thus the occurrence of paroxysmal bundle branch block of supraventricular origin in many patients may be misdiagnosed as VT by these methods and must be considered a confounding factor.

Acknowledgments: The authors wish to express their appreciation to Kevin Price, B.S., Ryan Reeg, B.S., Colleen Hoover, B.S., and Barbara Nagrant, B.S. for their technical assistance in the cardiac electrophysiology laboratory, and Ms. Debbie Laird for preparation of this manuscript.

References

1. Fisher JD, Goldstein M, Ostrow E, et al. Maximal rate of tachycardia development: Sinus tachycardia with sudden exercise vs. spontaneous ventricular tachycardia. PACE 1983; 6:221–228.
2. Geibel A, Zehender M, Brugada P. Changes in cycle length at the onset of sustained tachycardias —Importance for antitachycardia pacing. Am Heart J 1988; 108:588–592.
3. Fromer M, Kus T, Dubuc M, et al. Oscillation of ventricular tachycardia cycles length. (abstract) PACE 1987; 10:451.
4. Nathan AW, Creamer JE, Davies DW, et al. Clini-

cal experience with a new versatile, software based, tachycardia reversion pacemaker. (abstract) J Am Coll Cardiol 1986; 7:184A.
5. Olson W, Bardy G. Cycle length and morphology at the onset of spontaneous ventricular tachycardia and fibrillation. (abstract) PACE 1986; 9:284.
6. Olson W, Bardy G, Mehra R, et al. Comparison of different onset and stability algorithms for detection of spontaneous ventricular arrhythmias. (abstract) PACE 1987; 10:439.
7. Olson W, Bardy G, Mehra R, et al. Onset and stability for ventricular tachycardia detection in an implantable pacer-cardioverter-defibrillator. IEEE Computers in Cardiol 1987; 34:167–170.
8. Tomaselli G, Scheinman M, Griffin J. The utility of timing algorithms for distinguishing ventricular from supraventricular tachycardias. (abstract) PACE 1987; 10:415.
9. Warren J, Martin RO. Clinical evaluation of automatic tachycardia diagnosis by an implanted device. (abstract) PACE 1986; 9:16.
10. Ripley KL, Bump TE, Arzbaecher RC. Evaluation of techniques for recognition of ventricular arrhythmias by implanted devices. IEEE Trans on Biomed Eng 1989; 36:618–624.
11. Tomaselli GF, Nielsen AP, Finke WL, et al. Morphologic differences of the endocardial electrogram in beats of sinus and ventricular origin. PACE 1988; 11:254–262.
12. Lin D, DiCarlo LA, Jenkins JM. Identification of ventricular tachycardia using intracavitary ventricular electrograms: Analysis of time and frequency domain patterns. PACE 1988; 11:1592–1606.
13. Pannizzo F, Furman S. Frequency spectra of ventricular tachycardia and sinus rhythm in human intracardiac electrograms–application to tachycardia detection for cardiac pacemakers. IEEE Trans on Biomed Eng 1988; 35:421–425.
14. Mirowski M, Mower MM, Reid PR. The automatic implantable defibrillator. Am Heart J 1980; 100:1089–1092.
15. Mirowski M, Mower MM, Reid PR, et al. The automatic implantable defibrillator: New modality for treatment of life-threatening ventricular arrhythmias. PACE 1982; 5:384–401.
16. Davies DW, Wainwright RJ, Tooley MA, et al. Detection of pathological tachycardia by analysis of electrogram morphology. PACE 1986; 9:200–208.
17. Langberg JL, Gibb WJ, Auslander DM, et al. Identification of ventricular tachycardia with use of the morphology of the endocardial electrogram. Circulation 1988; 77:1363–1369.
18. Santel D, Mehra R, Olson W, et al. Integrative algorithm for detection of ventricular tachyarrhythmias from the intracardiac electrogram. IEEE Computers in Cardiology 1987; 34:175–177.
19. Pannizzo F, Furman S. Pattern recognition for tachycardia detection: A comparison of methods. (abstract) PACE 1987; 10:999.
20. DiCarlo L, Lin D, Jenkins J. Analysis of time and frequency domain patterns to distinguish ventricular tachycardia from sinus rhythm using endocardial electrograms. (abstract) Circulation 1987; 76:280.
21. Tomaselli GF, Gibb WJ, Langberg JJ, et al. In vivo testing of a morphology based approach to cardiac rhythm identification. (abstract) Circulation 1987; 76:1116.
22. Jenkins J, Noh KH, Guezennec A, et al. Diagnosis of atrial fibrillation using electrograms from chronic leads: Evaluation of computer algorithms. PACE 1988; 11:622–631.
23. Throne RD, Jenkins JM, Winston SA, et al. Discrimination of retrograde from anterograde atrial activation using intracardiac electrogram waveform analysis. PACE 1989; 11:1622–1630.
24. Woodroofe M. Probability with Applications. New York, McGraw-Hill, 1975, p. 229.
25. DiCarlo LA. October 30, 1989. Personal communication.